Spectral Distribution of Energy Dissipation of Wind-Generated Waves due to Dominant Wave Breaking

IAN R. YOUNG

Swinburne University of Technology, Melbourne, Victoria, Australia

ALEXANDER V. BABANIN

Faculty of Engineering and Industrial Sciences, Swinburne University of Technology, Melbourne, Victoria, Australia

(Manuscript received 20 August 2004, in final form 27 May 2005)

ABSTRACT

This paper considers an experimental attempt to estimate the spectral distribution of the dissipation due to breaking of dominant waves. A field wave record with an approximately 50% dominant-breaking rate was analyzed. Segments of the record, comprising sequences of breaking waves, were used to obtain the "breaking spectrum," and segments of nonbreaking waves were used to obtain the "nonbreaking spectrum." The clear visible difference between the two spectra was attributed to the dissipation due to breaking. This assumption was supported by independent measurements of total dissipation of kinetic energy in the water column at the measurement location. It is shown that the dominant breaking causes energy dissipation throughout the entire spectrum at scales smaller than the spectral peak waves. The dissipation rate at each frequency is linear in terms of the wave spectral density at that frequency, with a correction for the directional spectral width. A formulation for the spectral dissipation function able to accommodate this effect is suggested. Directional spectra of the breaking and nonbreaking waves are also considered. It is shown that directional dissipation rates at oblique angles are higher than the dissipation in the main wave propagation direction.

1. Introduction

Since it was first proposed by Hasselmann (1960), the radiative transfer equation has been widely used in scientific studies and practical applications related to the evolution of wind-generated waves. In water of finite depth, this equation takes the following form (Komen et al. 1994):

$$\left[\frac{\partial}{\partial t} + (c_g + \mathbf{U})\frac{\partial}{\partial \mathbf{x}} - \nabla\Omega\frac{\partial}{\partial \mathbf{k}}\right]\frac{E}{\omega} = S_{\text{in}} + S_{\text{nl}} + S_{\text{ds}} + S_{\text{bf}}, \tag{1}$$

where the left-hand side represents the evolution of the wave action density E/ω as a result of the physical processes of atmospheric input from the wind, S_{in}; nonlinear interactions of various orders within the spectrum, S_{nl}; dissipation due to "whitecapping," S_{ds}; and decay due to bottom friction, S_{bf}. $E(f, k, \theta)$ is the directional spectrum, the wave frequency is represented by $f = (\omega/2\pi)$, the wavenumber by k, and the direction of propagation by θ. All of the source terms are functions of wavenumber-frequency direction as well as other parameters. Here $\mathbf{U}$ is the surface current and $\Omega(\mathbf{k})$ is the Doppler-shifted frequency $\Omega(\mathbf{k}) = \omega(k) + \mathbf{k} \cdot \mathbf{U}$.

The dissipation-due-to-breaking source (sink) term S_{ds} is the subject of the present paper. Knowledge of the other source terms, based on either experimental or analytical (or both) approaches, is incomplete but still rational. In contrast, understanding of the dissipation term remains poor. A number of theoretical and conjectural approaches have been attempted to predict the spectral dissipation function, but none of these have been experimentally validated. It is generally assumed that S_{ds} is a function of the wave spectrum E:

$$S_{\text{ds}}(f, k, \theta) \sim E(f, k, \theta)^n, \tag{2}$$

Corresponding author address: Dr. Alex Babanin, Faculty of Engineering and Industrial Sciences, Swinburne University of Technology, P.O. Box 218, Melbourne, VIC 3122, Australia.
E-mail: ababanin@swin.edu.au

but there is no agreement on whether or not the spectral dissipation S_{ds} (f, k, θ) is linear in terms of the spectrum $E(f, k, \theta)$ (i.e., whether $n = 1$ or $n > 1$).

Donelan and Yuan (1994) classified theoretical models of the spectral dissipation into three types: whitecap models, quasi-saturated models, and probability models. We would add a turbulent model class to this classification (Polnikov 1993, mentioned below). None of these models, however, deals with the physics of wave breaking, which governs the wave energy lost. This physics, to a major extent, is unknown. All the models try to relate either the unstable wave state prior to the breaking or the residual wave and turbulence features after the breaking, to the subsequent or preceded dissipation due to the breaking.

Of the models that consider the waves prior to the breaking, the first analytical type developed was a probability model suggested by Longuet-Higgins (1969) and further developed by Yuan et al. (1986) and Feng and Yeli (1992). All of these studies used the Gaussian distribution of surface elevations to predict the appearance of wave heights exceeding the height of the Stokes limiting wave or its limiting acceleration $g/2$ at the crest (g is the gravitational acceleration). Such waves were assumed to break until the wave height is reduced to a limiting value, and the difference was attributed to the dissipation. The limiting value used differed from, the extreme Stokes value (Longuet-Higgins 1969; Yuan et al. 1986) to the mean value at a particular frequency derived from the Phillips (1958) equilibrium spectrum $F(\omega) = \alpha g^2 \omega^{-5}$ (Feng and Yeli 1992), where α is the Phillips equilibrium constant and $F(\omega) = \int E(\omega, k, \theta) dk\, d\theta$. The dissipation was found to be a linear function of the wave spectrum:

$$S_{ds}(k) = -a_1 A_1(\omega, m_0, m_2, m_4)\Phi(k), \tag{3}$$

where $\Phi(k) = \int E(f, k, \theta) df\, d\theta$, a_1 is an experimental constant, and A_1 is a complex function of frequency ω and integral moments of the wave frequency spectrum $F(\omega)$:

$$m_i = \int_0^\infty \omega^i F(\omega)\, d\omega. \tag{4}$$

More recently, however, it has been shown that the waves do not necessarily have to reach the $g/2$ acceleration limit to break (Holthuijsen and Herbers 1986; Hwang et al. 1989; Liu and Babanin 2004). In addition, once they are breaking they do not stop at the Stokes limiting steepness but may keep loosing energy until their steepness is well below the Stokes limit and even below the mean wave steepness (Liu and Babanin 2004). Therefore, even though conceptually attractive, the probability models, as they have been derived, are not quantitatively plausible.

The second type of prior-to-breaking class of models is what Donelan and Yuan (1994) called the quasi-saturated models (Phillips 1985; Donelan and Pierson 1987). These models rely on the equilibrium range of the wave spectrum, where some sort of saturation exists for the wave spectral density. In this region, the input, the wave–wave interactions and the dissipation [deep-water version of (1)] are assumed to be in balance. Therefore, at each wave scale (wavenumber), any excessive energy contributed by combined wind input and nonlinear interaction fluxes, does not bring about spectral growth but wave breaking and can be interpreted as the spectral dissipation local in wavenumber space. Phillips (1985) found that such dissipation is cubic in terms of the spectral density:

$$S_{ds}(k) = -a_2 A_2(\omega, k)\Phi(k)^3. \tag{5}$$

As above, a_2 is an experimental constant and A_2 is a spectral function that, in this case, does not depend on the wave power spectrum (i.e., the dissipation is local in wavenumber space).

Donelan and Pierson (1987) added consideration of wave directionality to the energy balance of the equilibrium range, arguing that a simple balance between wind input and dissipation is not observed at large angles to the wind. They also separately considered dispersive (gravity and capillary) waves and nondispersive (gravity–capillary) waves, as the nature of breaking differs because of different speeds of propagation relative to wave groups. Donelan and Pierson (1987) obtained a local-in-wavenumber-space dissipation function, similar to (5), but their exponent n depends on the wave spectrum $\Phi(k)$ and wavenumber k. For a given $\Phi(k)$, $n(k)$ will depend on how far the wavenumber k is from k_0; $1/k_0 = \lambda_0 = 0.0173$ m, where λ_0 is a wavelength in the center of the capillary–gravity range (i.e., where the waves are nondispersive). According to Donelan and Pierson (1987), n can vary significantly and, for $\Phi(k) \sim k^{-4}$, $n \approx 1$–5. It is essential, however, that $n \approx 5$ in most ranges of interest—both for gravitational and capillary waves.

This model type has multiple shortcomings. First, the very concept of the quasi-saturated or equilibrium interval is now subjected to doubt (M. A. Donelan 2003, unpublished manuscript). Even if it exists, the level α of the saturation is not constant, but depends on environmental conditions (Babanin and Soloviev 1998a). Even more importantly, none of the source terms that shape the spectral balance are known explicitly and accurately enough to provide a reliable determination of the dis-

sipation as a residual sink term (see, e.g., Donelan et al. 2006) concerning alterations of the input fluxes at strong wind-forcing conditions). Also, a dissipation function based on the breaking of short waves in the equilibrium interval does not account for dissipation due to dominant wave breaking, near the spectral peak, which may be more severe and can be quite frequent (Banner et al. 2000; Babanin et al. 2001; Banner et al. 2002). Last, there is growing evidence that dominant waves and the breaking of dominant waves affect dissipation at smaller scales (Banner et al. 1989; Meza et al. 2000; Donelan 2001). Therefore, dissipation in the saturation interval will not be a local function in wavenumber space. This last effect is considered in the present paper.

The most mathematically well-advanced and most frequently utilized dissipation model is that of Hasselmann (1974). This is an after-breaking class model as it relies on the distribution of well-developed whitecaps situated on the forward faces of breaking waves. According to Hasselmann (1974), once there is an established random distribution of the whitecaps, it does not matter what caused the waves to break: the whitecaps on the forward slopes exert downward pressure on upward-moving water and therefore conduct negative work on the wave. This model produces a linear dissipation:

$$S_{\mathrm{ds}}(k) = -a_3\omega^2\Phi(k), \tag{6}$$

where a_3 is a constant for a given wave state. Here a_3 depends on integral properties of the wave spectrum and therefore this dissipation function is not local in wavenumber space (like the probability models mentioned above, the breaking is considered local in physical space).

Two main assumptions of the model are that the dissipation, even if it is strongly nonlinear locally, is weak in the mean and that the whitecaps and the underlying waves are in geometric similarity. Both assumptions are not always strictly accurate. Banner et al. (2000) and Babanin et al. (2001) investigated wave fields with over 10% dominant-breaking rates. In the present paper, we examine a 60% dominant-breaking case. It is not clear whether the weak-in-the-mean approach is still applicable in such circumstances, which are apparently a regular feature of wind seas.

The geometric similarity is also an approximation for real unsteady breakers. The whitecapping commences at some point on the incipient-breaking crest and then spreads laterally and longitudinally (Phillips et al. 2001) and may or may not satisfy the similarity assumption even in the mean. Therefore, both assumptions need experimental verification. We should also point out that, before the distribution of established whitecaps is formed and commence the negative work on the wave, some energy is already lost from the wave to form the whitecaps, which is not accounted for by the model.

Polnikov (1993) suggested another type of after-breaking model. He argued that, no matter what the cause of the breaking, the result is turbulence in the water. Therefore, to describe the wave energy dissipation, it is sufficient to find a link between the wave spectrum and the water turbulence spectrum. Polnikov solved Reynold's equation where the Reynold's stress was expanded into a series with respect to velocity components and their spatial derivatives. The Prandtl mixing-length hypothesis was used to close the turbulent terms in these series. Polnikov found that the dissipation should be quadratic in the spectrum:

$$S_{\mathrm{ds}}(k) = -a_4A_4(\omega, U)\Phi(k)^2, \tag{7}$$

where, as above, a_4 and A_4 are a tuning constant and a spectral function, respectively, and $U(\omega)$ is the velocity field. By definition, this dissipation is local in wavenumber space.

Again, the idea is attractive, but the theory needs further development. The Reynold's equations are not directly applicable in a spectral sense, and the results are effectively obtained for monochromatic waves. Polnikov (1993) assumes that monochromatic waves are in fact spectral components of the continuous spectrum, as are the generated turbulent vortexes at respective scales. However, spectral waves of different scales interact, and the turbulent vortexes of particular scales are not only generated as a result of dissipation of counterpart waves, but also as a result of the collapse of larger vortexes (e.g., the Kolmogorov cascade).

Most important is that generation of the turbulence is not the only outcome of dissipation of wave energy. Melville et al. (1992) showed that 30%–50% of energy lost by breaking waves is expended on entraining bubbles into the water against buoyancy forces. This contribution, relative to the turbulence generation, is not constant across the spectrum. For example, microscale breakers do not cause air entrainment and therefore should expend relatively more energy on generating the turbulence.

To summarize this brief overview of existing theories of spectral dissipation, we find several studies that offer four different analytical models. None of the models deals with the dynamics of wave breaking, which is responsible for dissipation. Rather, they suggest hypotheses to interpret either prebreaking or postbreaking

wave field properties. All of the hypotheses lack experimental support or validation. Results vary from the dissipation being a linear function of the wave spectrum to the dissipation being quadratic, cubic, or even a function of the spectrum to the fifth power. In addition, some formulations represent the dissipation as being local in wavenumber space while others assume it is local in physical space.

Experimental confirmation should be an important element of the development of a theory. There have, however, been few experimental studies of wave dissipation. Thorpe (1993), Melville (1994), Terray et al. (1996), Hanson and Phillips (1999), among others, addressed the total dissipation. Very few field experimental studies: Donelan (2001), Phillips et al. (2001), Melville and Matusov (2002), and/or Hwang and Wang (2004) have attempted to obtain an experimental spectral dissipation function, and those attempts are indirect and not based on estimates of wave energy loss due to breaking.

Phillips et al. (2001) used high-range-resolution radar measurements and Melville and Matusov (2002) used aerial imaging to study distributions of the length of breaking wave fronts $\Lambda(c)$, where $\Lambda(c)dc$ is the average length of breaking crests per unit area of ocean surface traveling at velocities from c to $c + dc$ (Phillips 1985). They inferred a spectral function for the dissipation in terms of the phase speed c as the spectral parameter. Phillips et al. (2001) obtained it for a single wind speed and Melville and Matusov (2002) included a wind dependence into this function:

$$S_{\mathrm{ds}}(c) = -b\rho_w g^{-1} c^5 \Lambda(c)\left(\frac{10}{U_{10}}\right)^3, \tag{8}$$

where the wind speed U_{10} has to be expressed in meters per second. Connection of this dissipation with the wave spectrum was not obtained explicitly and therefore it cannot be directly compared with other dissipation functions above.

Donelan (2001) [as did Phillips (1985) and Donelan and Pierson (1987) in analytical models described above (5)], used the balance (1) to derive S_{ds}. He convincingly argued that, for stationary fetch-limited no-current conditions, S_{in} and S_{ds} are more than an order of magnitude larger than the advection and the nonlinear interaction terms. Therefore, there are wavenumbers in the wave spectrum $\Phi(k)$, where the balance is totally dominated by the wind input and the dissipation. If spectra of young fetch-limited waves are considered and an appropriate hypothesis about the form of the dissipation function is used, the spectral dissipation can be obtained from the spectral wind input function. Using only peak values of his spectra, Donelan (2001) obtained the dissipation as

$$S_{\mathrm{ds}}(k) = -36\omega(k)\Phi(k)B(k)^{2.5} \sim \Phi(k)^{3.5}, \tag{9}$$

where $B(k) = k^4\Phi(k)$ is termed the saturation spectrum. In (9), the dissipation remains local in wavenumber space. It is worth mentioning that, if the nonlinear interactions are not insignificant as was assumed, the result should not change qualitatively but will only be adjusted quantitatively since, according to Phillips (1985), S_{in}, S_{ds}, and S_{nl} should be proportional in the equilibrium range.

However, once Donelan (2001) applied (9) to the measured spectra at wavenumbers above the spectral peak, the S_{in} and S_{ds} balance could not be satisfied. The two energy source functions could only be brought into balance by assuming that the mean-square slope (MSS) of long waves modifies the dissipation rate at shorter waves. The dissipation function was adjusted accordingly:

$$S_{\mathrm{ds}}(k) = -36\omega(k)\Phi(k)\{[1 + \mathrm{MSS}(k)]^2 B(k)\}^{2.5}. \tag{10}$$

The dissipation (10) is not local in wavenumber space, due to the MSS term, as the quasi-saturated theories suggested, but on the contrary, acknowledges the importance of longer waves on the dissipation of short waves.

This influence, according to Donelan (2001) is due to the fact that dissipation rates for the short quasi-saturated waves are modulated by the straining action of longer waves. On the forward faces of longer waves, the short-wave steepness increases causing frequent breaking and correspondingly a net reduction in the energy density.

Apart from this plausible mechanism for longer waves affecting dissipation at shorter scales, other mechanisms have also been suggested by experimentalists. The other mechanisms involve effects due to breaking of large waves. Banner et al. (1989) showed that the large-scale breaking brings about rapid attenuation of short waves in its wake and therefore may cause the spectral dissipation function to depend on frequency relative to the peak. Meza et al. (2000), in a laboratory experiment with forced isolated breakers within transient wave trains, showed that dominant breakers do not cause energy loss from dominant waves, but almost exclusively from wave components well above the spectral peak.

Hwang and Wang (2004), like Donelan (2001), used the source term balance (1) idea to derive S_{ds}, but they applied this approach to spectra of short waves, at least

twice the peak frequency, with wavelengths from 6 to 2 cm. Their results are very peculiar, with the dissipation proportional to $B^{2.3}$ for capillary waves, approaching B^3 at the other end of the scale, and reaching up to B^{10} in the middle wavelength range. Hwang and Wang (2004) did not obtain the cumulative term which is a part of the parameterization (10) and is also a result of the present paper. In fact, they could not obtain such a dependence, having based their balance closure on a local-in-wavenumber-space dissipation approach. However, if the large-scale breaking was present in Hwang and Wang (2004) data, then the cumulative term may become noticeable and may be responsible for the sharp rise of their dissipation in the middle range of their wavelengths.

Hence, the experimental evidence indicates that the dissipation function is, most likely, not local in wavenumber space and is a function of the wave spectrum. However, the experiments, do not support any of the suggested theoretical forms for the dissipation. These studies yield different conclusions as to the mechanisms by which dominant waves affect smaller-scale dissipation. Banner et al. (1989) and Meza et al. (2000) attribute the effect to breaking waves, whereas, Donelan (2001) attributes the effect to nonbreaking waves. There are also different conclusions as to the magnitude of the effect: from no effect (Meza et al. 2000) to $S_{ds}(k) \sim \Phi(k)^{3.5}$ in (10) according to Donelan (2001).

All of the studies described above have been aimed at determining the dissipation source term required to produce known spectral forms. However, an alternative theory, which does not require detailed knowledge of the dissipation has also been developed (Zakharov 1966, 1968, 2002; Zakharov and Filonenko 1967; Zakharov and Smilga 1981; Zakharov and Zaslavskii 1982a,b, 1983a,b; Kitaigorodskii 1983). In their theory of weak turbulence, Zakharov and his colleagues obtain a Kolmogorov spectrum of $F(\omega) \sim \omega^{-4}$ as an exact solution of the kinetic equation for gravity waves in the equilibrium interval. This spectrum agrees with many experimental observations (Toba 1972; Kahma 1981; Leykin and Rozenberg 1984; Donelan et al. 1985, among others). In addition, Zakharov (2002) was able to reproduce known growth curves of wave integral properties as analytical solutions on the basis of the theory of weak turbulence.

This theory relies on the assumption that the whitecap dissipation can be neglected in the frequency range of the spectral peak and the universal region at wavenumbers above the peak. This assumption is not obvious, as the dominant waves are known to break, sometimes quite frequently (Banner et al. 2000, 2002; Babanin et al. 2001). There is contradictory experimental evidence regarding the effect that dominant breaking has on wave spectral peak dissipation (Meza et al. 2000; Donelan 2001, mentioned above).

The current paper was stimulated by Zakharov's presentation at the eighth Waves in Shallow Environment meeting (WISE-8), Toronto, Canada, in 2001, and was aimed at direct measurement of the spectral dissipation due to dominant breaking for wind-generated waves. This was done for a field record with a near 50% dominant-breaking rate (dominant breaking is defined in the next section). The approach adopted compares spectra of breaking waves and nonbreaking waves occurring within a single record with stationary and homogeneous wind–wave conditions. Section 2 describes the approach and section 3 provides a verification of the approach by independent means. Sections 4 and 5 address the main results—determination of the spectral dissipation due to dominant breaking—in both frequency and direction. Section 6 summarizes the conclusions and suggests a function for the frequency spectral dissipation.

2. The approach

As described in section 1, since the physics of wave energy transformation during breaking is unknown, the previous attempts to obtain the spectral dissipation function have been based on indirect interpretations of assumed properties of waves. These properties were considered either prior to breaking or after breaking. Alternatively, approaches based on the assumed balance with the better-known input have also been used. A more direct experimental approach is attempted in the present paper. In a stationary fully developed (in finite depth) wave field, spectra of incipient dominant-breaking wave trains (i.e., sequences of dominant waves within which almost every dominant wave breaks) were compared with spectra of trains of dominant broken waves. The difference was attributed to the spectral dissipation due to the breaking of dominant waves.

The terminology "dominant breaking" requires definition. We call dominant waves those waves with frequencies $f = f_p \pm 0.3f_p$, where f_p is the spectral peak frequency, and correspondingly the dominant breakers will be breaking waves from this frequency range. The acoustic-spectrogram method of Babanin et al. (2001) can be used to detect the breakers in this range as described in section 2b. This method has been recently verified by an independent approach based on detecting individual bubble-formation events (Manasseh et al. 2006). This latter approach, having used the same wave data as the present study, closely confirmed the

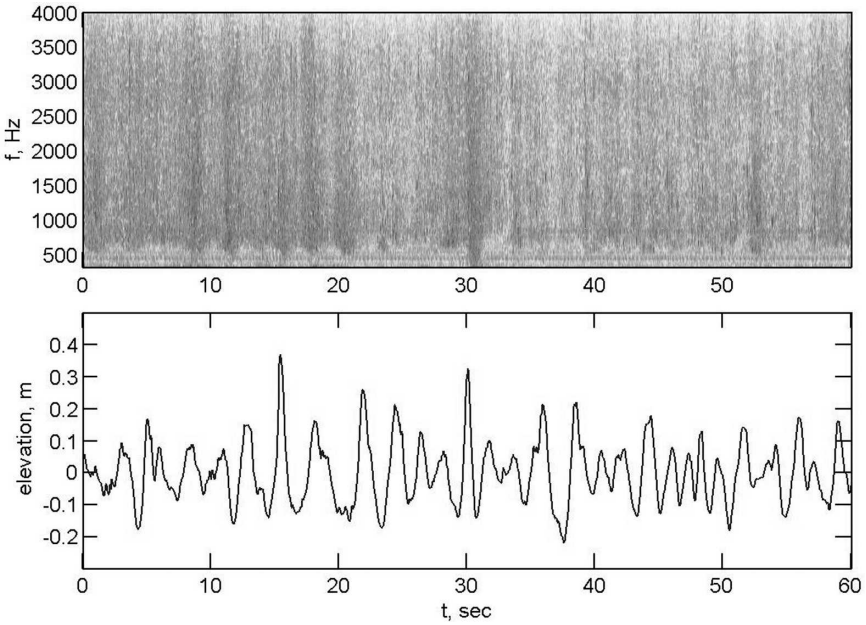

FIG. 1. (top) Spectrogram of acoustic noise of 1 min of the record. Dark crests are associated with breaking waves. (bottom) Synchronous surface elevation record.

breaking statistics obtained by Babanin et al. (2001) for the dominant-breaking waves.

Obviously, waves of scales smaller than those of the dominant wave also break. That breaking can be brought about by local processes once those shorter waves exceed some threshold properties as described in Banner et al. (2000), Babanin et al. (2001), and Banner at al. (2002), or can be induced by breaking of waves of larger scales. Dissipation at small wave scales due to the latter effect is linked to the larger breaking events and in this paper, where the dominant breaking is studied, such dissipation will be considered as a consequence of the breaking of dominant waves.

a. The experiment

The Australian Shallow Water Experiment (AUSWEX), carried out at Lake George in New South Wales in 1997–2000, was designed to simultaneously measure the major source and sink functions, including the dissipation, in situ, in a finite-depth environment (apart from the nonlinear interactions, which were to be computed). A comprehensive description of the experiment and relevant techniques, developed to detect and quantify the breaking events, has been given in Young et al. (2005). Here, we shall only briefly describe measurement and data-processing procedures pertinent to the present study.

The surface elevation records were gathered by an array of high-precision capacitance wave probes. Since wave-breaking criteria are not unambiguously established, and therefore visual detection of breaking occurrence is arguably the most reliable method available, the wave records were supplemented by videotaped images of the water surface surrounding the wave array. Both the surface elevation sampling and the video framing were performed at 25 Hz and synchronized. This approach enabled the authors to visually verify events on the water surface, used for the analysis.

A bottom-mounted hydrophone (water depth of 1.1 m), data from which was synchronized with the wave array, was used to detect and quantify breaking events. This method was developed in Babanin et al. (2001) and effectively allows the identification of individual breaking waves and trains of waves with enhanced intensity of breaking without need for repeated viewing of video images.

The top panel in Fig. 1 shows a spectrogram of 1 min of the sound record. The spectrogram is a time series of consecutive spectral densities computed over 256 readings of the acoustic signal with a 128-point overlap (the segments were windowed with a Hanning window). Values of the spectral density are shown using a logarithmic scale, with darker patches corresponding to higher values (i.e., louder recorded sound levels).

The dark crests across almost the entire 4-KHz frequency span in the spectrogram are associated with acoustic noise from dominant-breaking waves. This was confirmed through repeated viewing of the synchro-

nized video records (Babanin et al. 2001). The period of dominant waves for this record was 2.8 s and, as can be seen by comparing the spectrogram with the synchronous wave record in the bottom panel, almost all dominant waves in the first half-minute were breaking whereas hardly any of the dominant waves broke during the second half-minute.

High-frequency measurements of the water currents, also sampled at 25 Hz, and synchronized with the rest of the measurements, were carried out at the location of the wave array with a number of SonTek Acoustic Doppler Velocimeters (ADVs). Duration of a typical record was 20 min, as were the durations of recording for the other properties. A detailed description of the measurements is given in Young et al. (2005). Thus, velocity spectra of underwater turbulence were obtained. These spectra clearly exhibit the $\sim\omega^{-5/3}$ Kolmogorov subintervals of locally isotropic turbulence, and hence provide estimates of total dissipation rates ε, which are a function of the Kolmogorov interval level, at a measurement point (Terray et al. 1996; Veron and Melville 1999).

b. Segmenting procedure

For the analysis, a wave record with an approximately 60% dominant-breaking rate was chosen. This was as close as we could get to a 50% rate, which would mean that half of the time waves within a single stationary record were breaking and half of the time waves were recovering from the breaking loss. The 50% division of the record into breaking/nonbreaking parts enabled us to estimate spectra of breaking and nonbreaking waves with similar confidence intervals, as will be described below. The waves were stationary (scatter of 1-min standard deviation surface elevation, relative to the 20-min mean, was less than 10%, with no drift of the mean) under steady $U_{10} = 19.8$ m s^{-1} wind (measured at 10-m height), with peak frequency $f_p = 0.36$ Hz and significant wave height $H_s = 0.45$ m. The parameterization of Young and Verhagen (1996) was used to verify that the waves were fully developed in the bottom-limited environment with the measured depth, $d = 1.1$ m. The wave record was 20 min long and was segmented into five breaking parts and four nonbreaking parts.

In this highly forced situation, approximately half the waves are actively breaking. It is assumed that those waves not breaking, have recently done so, having lost their energy in the breaking process. This assumption seems reasonable in this highly forced environment and the analysis that follows is predicated on this assumption.

Models of wind waves, both physical and numerical, implicitly accept a double-scale approach to the wave field (see, e.g., Melville 1994). At long scales of thousands of wavelengths and periods, the waves are assumed to be evolving. In a general case, at this scale the left-hand-side derivative in (1) is positive as the waves grow under wind forcing. If the wave field is stationary and characterized by constant-depth (or deep) conditions, the evolution along the wave fetch is described by the advective term on the left-hand side of (1) which is small [less than 5% according to Donelan (2001)] relative to the wind input S_{in} and the dissipation S_{ds} on the right-hand side. The magnitude of the nonlinear term S_{nl} is also small if compared with S_{in} and S_{ds}, but the energy transfer across the spectrum becomes essential at the scales of thousands and tens of thousands of wave periods (Hasselmann 1962; Zakharov 1968). In our case of a stationary fully developed constant-depth wave environment, the full derivative is zero and the right-hand-side terms of (1) are balanced.

At medium scales of hundreds of wavelengths, the wave fields are usually assumed to be stationary and homogeneous. Sequences of such waves are used to obtain statistically reliable estimates of wave spectra in experiments and spectra of this scale are used in wave forecast and research spectral models. Such models have been reasonably successful and this, to some extent, justifies the assumption.

Indeed, the small advective and S_{nl} terms are not capable of bringing about significant changes to the wave spectrum at such time scales. For the dissipation term controlled by wave breaking, however, the scale of hundreds of waves is not small. For example, laboratory experiments on unsteady deep-water breaking by Rapp and Melville (1990) show that the breaking is a rapid process of the same order of magnitude in time as the wave period and causes a 10%–25% energy loss from the wave group where the breaking occurs. If, within the measurement time span of hundreds of waves, each wave breaks even once, changes to the spectrum will be significant. Such dramatic losses of energy are, however, not observed at these time scales since the breaking rates are usually not very large (Holthuijsen and Herbers 1986; Banner et al. 2000, among others) and, at this time scale, the wind input is apparently capable of restoring the mean spectrum after breaking. This also means that, at this time scale, energy input by the wind is a slower process than the energy loss from breaking, as the energy is input to every wave in the field, whereas it is only lost from a fraction of the waves.

Spectral models based on the medium-scale averaging of the wave field may have reached their limit in

accuracy with which they can simulate realistic wave generation and growth conditions (Liu et al. 2002). This can be, in part, due to the fact that they average out variations of the wave field at scales of several waves (wave group scale). It is this shorter-scale group structure that may play a major role in intermittent wave breaking (Donelan et al. 1972; Holthuijsen and Herbers 1986; Banner et al. 2000) and modulation of the wind stress (Skafel and Donelan 1997). There is modulation of the surface roughness at even shorter scales of dominant waves (Kudryavtsev and Makin 2002; Hara and Belcher 2002) and disregarding this effect in models of wave growth can lead to underestimation of the growth rate parameter by a factor of 2–3 when compared with measured values. The spectral equation in (1) is not designed for applications at times scales of individual waves and wave groups.

What happens at the scales of dozens of waves or a hundred waves? In the case of normal weak-in-the-mean breaking conditions, there should be not much variation in properties at this scale. In the case investigated here, the strongly forced and frequently breaking dominant waves come in alternating breaking and nonbreaking trains from 4 to 120 dominant waves long. The breaking waves are, on average, significantly higher and steeper than those not breaking (Holthuijsen and Herbers 1986). Therefore, it is expected that there will be a noticeable difference between the spectra calculated over breaking wave train segments and the spectra over nonbreaking segments.

Since breaking is the only major process to contribute to the rapid dissipation at this time scale (the bottom friction is relatively small and also relatively constant across the breaking/nonbreaking segments), the difference can be attributed to dissipation due to the breaking of the dominant waves in the spectrum. This difference will constitute a nonzero term on the right-hand side of (1). The main assumption of this paper is that the difference can be attributed to only the partial derivative and the advective term is small. An assumption regarding the advective term was needed as it was not possible to directly measure its value. The waves were measured using a spatial array of wave probes with the largest separation of 30 cm between the probes (Young et al. 2005). At such distances, spectral difference along the wave fetch (between the probes) was negligible and could not be detected with any degree of confidence. It may mean that the advection is small but, since this distance is only a fraction of the dominant wavelength, any spectral difference could have been buried within the statistical scatter. Thus, to determine the spectral energy loss due to dominant breaking, it was assumed that it should be sufficient to measure differences between the spectra of breaking and nonbreaking waves based on measurements of the time series at a point.

This difference will be a lower-bound estimate of the dissipation due to breaking. The approach treats the segments of breaking waves as a sequence of incipient breakers. In fact, waves breaking at the measurement point already exhibit some whitecapping and therefore they have already lost some energy prior to arriving at the measurement point. The broken waves in the nonbreaking sequence are already gaining energy from the wind, but this energy is still not sufficient, on average, to bring them to the breaking point. Also, the breaking waves are at the same time receiving energy from the wind. This means that the wind input rate is still slower relative to the dissipation, but growth rates and breaking dissipation rates are now comparable and differ only by 2–3 times. This interesting observation indirectly supports the conclusion made in Donelan et al. (2006) that the growth rates depend on the wave steepness.

To summarize the segmenting approach described above, we would mention again that, in the wave record with a 60% dominant-breaking rate, we will treat the trains of dominant breakers as sequences of incipient breakers and the trains of nonbreaking waves as sequences of waves that have just broken. This will lead us to a lower-bound estimate of the dominant-breaking impact across the spectrum. Thus, there will be multiple segments of wave record, from 0.5 min to a few minutes long, used to obtain spectra based on these individual segments. The spectra obtained for breaking segments and those obtained for nonbreaking segments will then be averaged to produce reliable estimates of the *incipient-breaking* spectrum and of the *postbreaking* spectrum.

The method described in Babanin et al. (2001) can be used to segment the wave records. Spectrograms of acoustic noise recorded by the hydrophone clearly demonstrate patches of enhanced and lowered noise level, which were shown to be associated with breaking activity of dominant waves at the wave measurement spot above the hydrophone. For example, in Fig. 1 the first 35 s would be an incipient-breaking segment and the last 25 s, a postbreaking segment.

c. *Spectra of incipient-breaking and postbreaking waves*

The spectrogram method was used to segment the wave record with a nearly 50% dominant-breaking rate and to obtain a mean incipient-breaking spectrum $F_i(f)$ and a mean postbreaking spectrum $F_p(f)$ within this

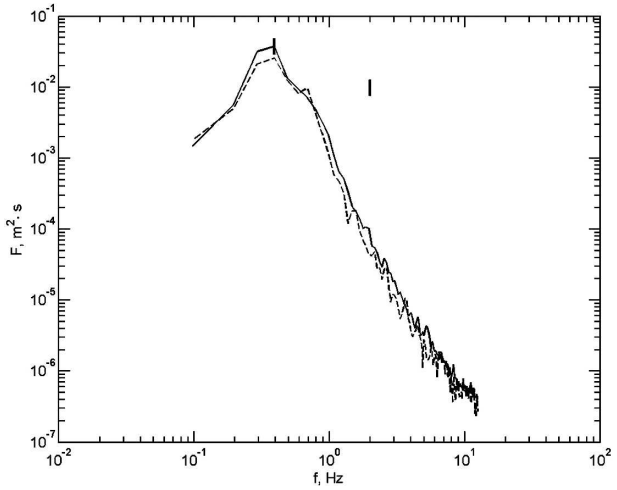

FIG. 2. Mean power spectrum of incipient-breaking (solid line) and postbreaking (dashed line) waves. The 95% confidence limits are shown.

record with the same confidence intervals. The two spectra are shown in Fig. 2. There is a clear difference between the spectra, with $F_p(f)$ having consistently lower spectral density as one would expect. Confidence limits are very small, and overall the spectra of broken waves lie below the 95% confidence limits of the spectra of nonbreaking waves. The higher-order moments also exhibit interesting differences:

$$\begin{aligned} \text{skewness}_i &= 0.45, \\ \text{skewness}_p &= 0.31, \\ \text{kurtosis}_i &= 3.34, \\ \text{kurtosis}_p &= 2.96, \\ \text{asymmetry}_i &= -0.186, \quad \text{and} \\ \text{asymmetry}_p &= -0.017. \end{aligned} \tag{11}$$

The nonbreaking waves in this strongly forced situation have quite high skewness and kurtosis. The breaking waves are even more skewed whereas their kurtosis is only just higher. There is a possibility that, because of the difference in skewness between breaking and nonbreaking waves, there will be a difference in surface orbital velocities and therefore in Doppler shifts between the breaking and nonbreaking segments. These effects were estimated and were found negligible. The difference in asymmetry is remarkable: nonbreaking waves are, approximately, symmetric, whereas their breaking counterparts show very strong asymmetry.

The spectral difference is quantified in the bottom panel in Fig. 3, where the ratio of the two spectra is plotted as a function of frequency *f*. The top subplot duplicates Fig. 2 to make comparisons easier. Clearly, the loss of spectral density, following the breaking of dominant waves, is spread across almost the entire frequency range. Although there is considerable noise, the

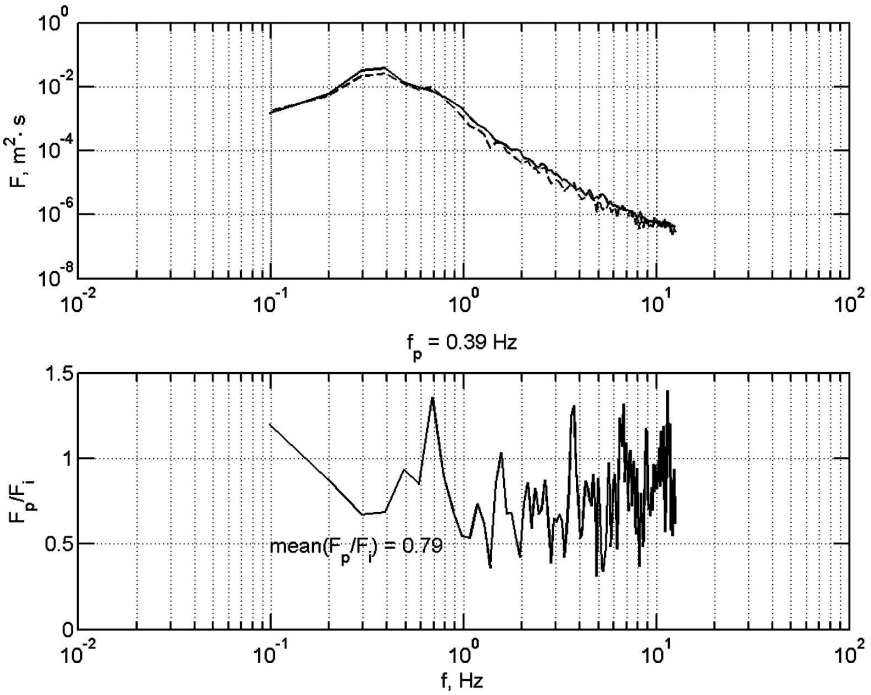

FIG. 3. (top) Mean power spectrum of incipient-breaking (solid line) and postbreaking (dashed line) waves. (bottom) Ratio of the spectra shown in top panel.

longer wave scales appear to be more affected by the dominant breaking, than the shorter scales of $f > 5f_p$. It is possible that these shorter scales recover from the breaking impact at a time scale of a few tens of dominant periods (shorter than the averaging period of the spectra shown here). As our reviewer pointed out, it is also possible that the broadband impact of the dominant breaking becomes less effective at high frequencies. The strongest attenuation is observed for waves in the $3f_p$–$5f_p$ range. The mean energy loss across the full measured spectrum is approximately 20%.

It has to be emphasized here that, even though the short waves do also break as mentioned above, the observed broadband difference of the two spectra is due to the dominant breaking. The inherent breaking of short waves, which would naturally occur in the absence of background dominant breaking, would not be detected by the segmenting method. Such breaking will randomly occur on a time scale shorter than the segment length. As a result, such smaller-scale breaking will occur in all segments and the resulting differences in the energy between the segments will not identify breaking at this scale. Therefore, any differences in the high-frequency parts of the spectra are linked to dominant breaking, rather than to processes actually occurring at the higher frequencies.

The fact that breaking of the dominant waves causes dissipation across the full spectrum is not totally unexpected and impacts some of the considerations in section 1. If the breaking is local in wavenumber space, as some approaches assume (Donelan and Pierson 1987; Polnikov 1993), then one would expect the energy loss to be concentrated around the spectral peak. Clearly, this is not the case. Also, the laboratory results of Meza et al. (2000), where forced breakers within transient wave trains caused energy loss almost exclusively from wave components well above the spectral peak, does not agree with the observed results under these field conditions.

In the interpretation adopted here, it is assumed that the breaking event is a local disturbance in the physical space. This assumption may not be strictly correct. According to Donelan and Yuan (1994), such an assumption would lead to a white spectral distribution of the dissipation in the wavenumber domain. As shown in Fig. 3, this is not the case, with the dissipation depending on the local wave spectrum density, rather than having a white distribution. Perhaps, Banner et al.'s (1989) attenuation of short waves in the wake of larger breakers is a possible candidate. Such speculation of the actual physical process active in the breaking is, however, beyond the scope of this paper.

3. Verification of the approach

The assumption that the difference between the observed spectra in Figs. 2 and 3 are due to dominant breaking require quantitative verification. Measurements of the total dissipation in the water column beneath the surface waves were used for this purpose. Estimates obtained by means of such measurements are not necessarily more accurate than the estimates obtained below by the segmenting method, but the first approach is quite well established and provides a good reference value for our results.

The volumetric rate of total turbulent kinetic energy dissipation ε can be obtained from the Kolmogorov inertial subrange of the velocity spectrum in the water (Terray et al. 1996; Veron and Melville 1999). If the velocity spectrum $V(f)$ exhibits an $f^{-5/3}$ Kolmogorov interval, the level of this interval depends on the dissipation ε:

$$V(f) = \frac{7}{110}\,2^{(4/3)}\Gamma\left(\frac{1}{3}\right)\left(\frac{8\varepsilon}{9\alpha}\,\frac{u_{\mathrm{rms}}^{\mathrm{orb}}}{2\pi}\right)^{2/3} f^{-(5/3)}, \quad (12)$$

where $u_{\mathrm{rms}}^{\mathrm{orb}}$ is the rms orbital velocity and $\alpha \approx 0.4$ is Heisenberg's constant (Veron and Melville 1999). The larger the dissipation rate ε, the higher the Kolmogorov interval of the spectrum $V(f)$.

Here ε is the dissipation rate per unit of volume, and to obtain the total dissipation in the water column per unit of area, D one needs to integrate $\varepsilon(z)$ over the water depth z from the surface $z = 0$ to the bottom $z = d$:

$$D = \int_0^d \varepsilon(z)\,dz. \quad (13)$$

To perform the integration, either continuous measurements of the $\varepsilon(z)$ profile or its parameterization with depth are required. Knowledge of the parameterization is obviously preferable as it enables estimation of the total dissipation on the basis of a single-depth measurement of the spectrum in (12).

There is, however, no general agreement on the parameterization of the vertical dissipation distribution $\varepsilon(z)$. In the classical theory of the boundary layer over a solid wall, ε is a linear function of the distance z to the wall (see, e.g., Landau and Lifshitz 1986). Early measurements in the boundary layer beneath the wavy surface found the ε-depth distribution to be consistent with this wall-layer theory (Arsenyev et al. 1975; Dillon et al. 1981; Oakey and Elliott 1982; Jones 1985; Soloviev et al. 1988). More recently, however, by both direct and indirect means it was shown that, at least at strong wind forcing, the dissipation ε close to the water surface

may exceed the wall-layer values by up to two orders of magnitude (Agrawal et al. 1992; Melville 1994; Terray et al. 1996; Drennan et al. 1996). Terray et al. (1996) and Drennan et al. (1996) parameterized the vertical dissipation profile as

$$\varepsilon(z) = \begin{cases} \text{const} & z < H, \\ z^{-2} & z \geq H. \end{cases} \tag{14}$$

Based on considerations of the expected total wind input that should match the total dissipation, it was found that H approximately scales with significant wave height H_s as $H = 0.6H_s$ (Terray et al. 1996; Drennan et al. 1996). Recent refined studies of Soloviev and Lukas (2003) and Gemmrich and Farmer (2004) confirmed the existence of enhanced near-surface turbulence due to breaking, but pointed out that the scaling H of the constant-dissipation level is still an issue.

At Lake George, turbulence spectra $V(f)$ were measured by ADVs as mentioned in section 2a and described in Young et al. (2005) in greater detail. Under strong wind forcing, such spectra exhibited distinct Kolmogorov intervals as shown in Fig. 4. Dissipation rates ε obtained on the basis of such spectra using (12) are shown in Fig. 5. Figure 5 shows $\varepsilon\kappa z/u_{*w}^3$ plotted as a function of gz/u_{*w}^2, where u_{*w} is the friction velocity in the water and $\kappa \approx 0.4$ is the von Kármán constant. Wall-law scaling is applied to the dissipation ε and the scaling height of fully developed waves is applied to the water depth z (see Agrawal et al. 1992; Melville 1994). For boundary layers over solid walls, such scaling of the dissipation would give values of $\varepsilon\kappa z/u_{*w}^3 = 1$ shown by the vertical line in the figure. The scatter, particularly close to the surface, is large which is due to undersampling of the intermittent turbulent field (Melville 1994). However, the enhancement of the dissipation rates, when compared with the wall layer, is obvious. Maximum values of enhancement are up to 200 times the wall-layer values [even greater than those in Agrawal et al. (1992), in which they were up to 70 times], and therefore a quadratic dissipation profile, as described by (14), is expected for such circumstances.

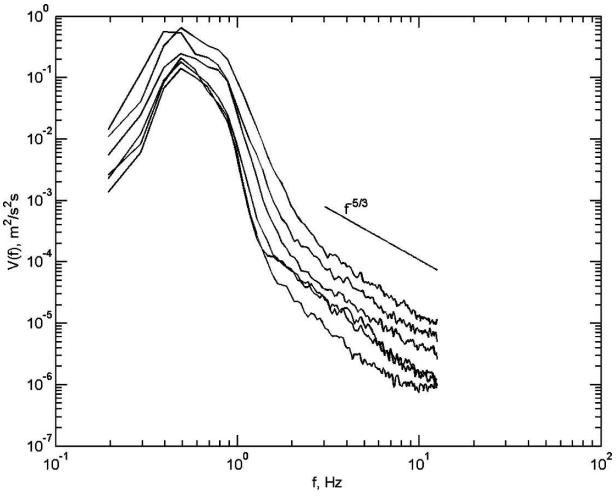

FIG. 4. Velocity spectrum $V(f)$ measured at 10-, 20-, 30-, 40-, 50-, and 60-cm distances from the surface for a 9.7 m s^{-1} mean wind speed (the more energetic spectra are closer to the surface). The Kolmogorov interval slope of $f^{-5/3}$ is shown.

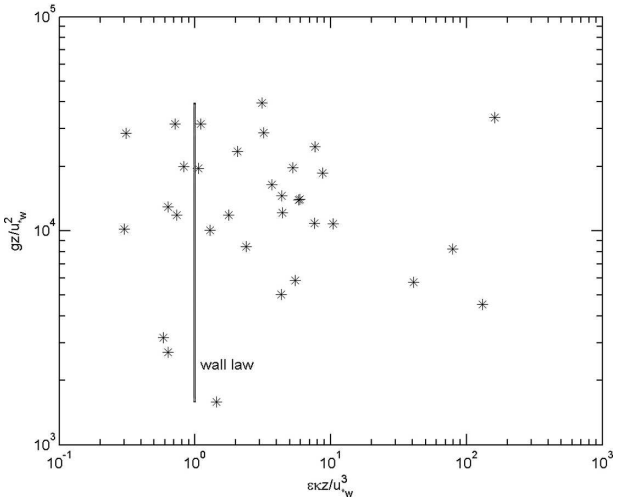

FIG. 5. Dissipation ε vs depth z in the wall-layer coordinates (section 3). The vertical line represents the dissipation level in the boundary layer over a solid wall.

The vertical profile of the turbulent spectra presented here was obtained by means of a high-precision ADV (Young et al. 2005). The ADV was traversed down from the surface in 10-cm increments and the six 20-min spectra shown in Fig. 4 were recorded at 10, 20, 30, 40, 50, and 60 cm from the mean water level, respectively. The wind was steady in speed and direction over the 2-h time period of measuring the profile, $U_{10} = 9.7$ m s^{-1} on average, with a maximum of 10.9 m s^{-1} and a minimum of 8.3 m s^{-1}. The more energetic spectra shown in Fig. 4 were recorded closer to the surface, with the energy level decaying with depth.

The vertical profile of ε is shown in Fig. 6. The profile is very close to quadratic and therefore parameterization of (14) was subsequently used to estimate the total dissipation D. In our estimates, $H = 0.25H_s$ was chosen. This value was obtained from comparisons of the total dissipation with the total wind input on the basis of Lake George data. The wind input, used for the comparisons, was measured simultaneously with the dissipation (Donelan et al. 2006). This directly measured relationship was preferred to $H = 0.6H_s$ proposed by Terray et al. (1996) and Drennan et al. (1996), which

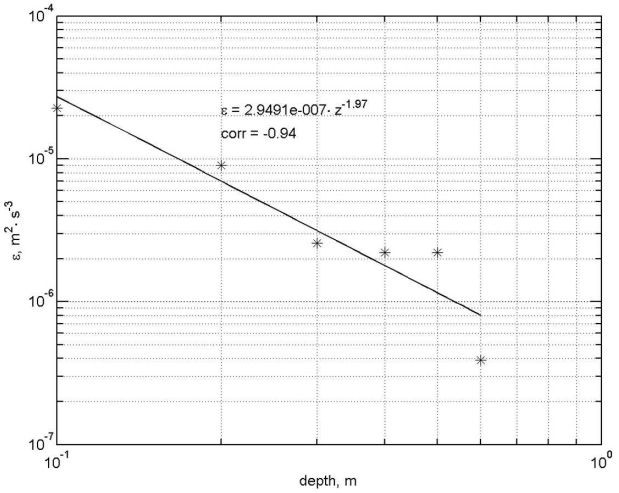

FIG. 6. Dimensional profile of dissipation ε vs depth z, obtained from turbulence spectra shown in Fig. 4. The line of best fit and its correlation coefficient are shown.

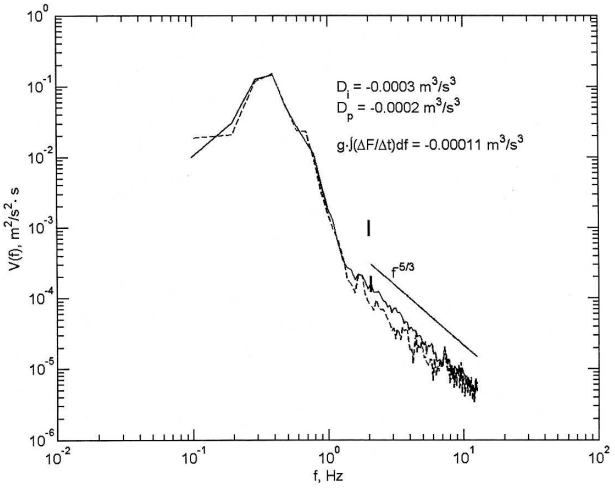

FIG. 7. Mean velocity spectrum of incipient-breaking (solid line) and postbreaking (dashed line) waves. The Kolmogorov interval slope of $f^{-5/3}$ is shown. The text shows values of respective total dissipation rates in (13) and the integral of spectral dissipation seen in Fig. 2. The 95% confidence limits are shown.

was based on an inferred total wind input as described above. The simultaneous measurements of the total dissipation and the wind input and their comparisons are the subject of a separate paper and therefore will not be discussed further.

Therefore, the quadratic dissipation profile for the strong-wind Lake George records was adopted. During the wave record analyzed in the present paper, synchronized ADV measurements were carried out at a distance of 20 cm from the surface at the location of wave array. ADV velocity spectra of incipient-breaking and postbreaking periods are shown in Fig. 7. The orbital velocities of waves from the two periods (peak values) do not appear to differ significantly. The levels of the Kolmogorov intervals of the two spectra are, however, dramatically different. This difference can be attributed to the loss of energy from across the wave spectrum seen in Figs. 2 and 3. The total dissipation estimated from the velocity spectra and the wave spectra should match

$$D_i - D_p = g \int_f \overline{\left[\frac{F(f)_p - F(f)_i}{\Delta t}\right]} df, \qquad (15)$$

where Δt is the time difference between the mean time points of subsequent breaking and nonbreaking segments and the overline represents the ensemble average. Here and subsequently, the spectral dissipation term will be multiplied by g: $S_{ds} = g(\Delta F/\Delta t)$ rather than $S_{ds} = \Delta F/\Delta t$ as follows from (1). This is done to match the dimensions of dissipations D and $\int_f S_{ds}(f)\, df$.

Based on the data in Fig. 7, [using (13)] under the incipient dominant breakers, the dissipation rate per unit of area is $D_i = -0.0003\ \text{m}^3\ \text{s}^{-3}$, and under the broken dominant waves it is $D_p = -0.0002\ \text{m}^3\ \text{s}^{-3}$. The latter, of course, should not be zero in the absence of dominant breaking because dissipation due to breaking of waves of all other scales persists. The difference $D_i - D_p = -0.0001\ \text{m}^3\ \text{s}^{-3}$ matches remarkably well the integral $g \int_f (\Delta F/\Delta t)\, df = -0.000\,11\ \text{m}^3\ \text{s}^{-3}$. Although this is a pleasing result, it should be remembered that both approaches yield only an approximate estimate of the dissipation.

As mentioned in sections 2b and 2c, the spectral difference in Fig. 2 is a lower-bound estimate of dissipation due to the breaking, because some energy must have already been lost before the spectra were measured. The difference $D_i - D_p$ of the total dissipation rates of kinetic energy is also likely to be a lower-bound estimate of the loss of energy from the wave field due to breaking. As mentioned above, some of the energy is expended on work against buoyancy forces while entraining bubbles into the water, rather than on generating the turbulence. The fraction of the wave energy dissipated, which is expended in entraining the air can be up to 30%–50% of the total (Melville et al. 1992) and this defines the limits of the accuracy of our segmenting method. For the laboratory measurements of Melville et al. (1992) some of the breaking was of a plunging type. In contrast, most of the Lake George breaking was of the spilling type, which expends less energy on entrainment. Therefore, we would expect that in our case the fraction of energy expended this way is at the lower bound of 30% and perhaps even less

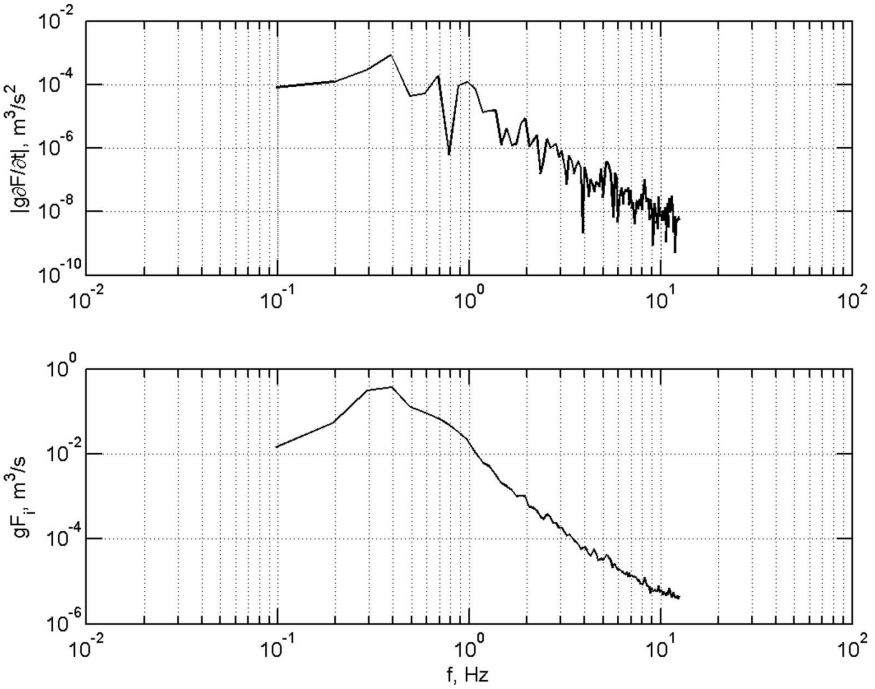

FIG. 8. (top) Spectral difference $[\Delta F(f)]/\Delta t$ in (16) as a function of frequency f. (bottom) The incipient-breaking spectrum $F_i(f)$.

than that. Nevertheless, the above comparison shows that the proposed method of estimation of wave-breaking dissipation by considering the difference between the incipient- and postbreaking spectra provides a reasonable estimate of the total dissipation. The accuracy probably being of the order of 30%. The quantitative verification of total dissipation does not independently validate the observed spectral distribution of the breaking effect, but the possible spectral bias must be within the 30% total accuracy.

One more interesting observation based on Fig. 7. Here, one can see that the orbital velocities of the dominant waves did not change between the breaking and nonbreaking segments. This implies that the energy, which is obviously gone from the power spectra, must have been the potential energy, rather than kinetic. What is important here is that the dominant orbital velocities are the same between the segments, and therefore the bottom friction is the same for the breaking and nonbreaking wave trains as was stated above.

4. Spectral dissipation due to dominant breaking in the frequency domain

The dissipation $S_{ds}(f, k, \theta)$, as described in section 1 above, is traditionally expressed as a power function of the wave spectrum $E(f, k, \theta)$ in (2). Similarly, we initially consider the spectral dissipation due to dominant breaking in terms of the omnidirectional frequency spectrum $F_i(f)$ of incipient breakers:

$$S_{ds}(f) = g\frac{\Delta F(f)}{\Delta t} \sim -[gF_i(f)]^n. \tag{16}$$

This expression can be made dimensionally consistent by using, for example, the mean frequency, as is done in some dissipation models. In our case, it would not change anything because we only used one record and the mean frequency would be a constant.

The spectral difference $g[\Delta F(f)]/\Delta t$ and the spectrum $F_i(f)$ are both plotted in Fig. 8. The features of the two spectral functions are visually similar and one would expect a linear relationship between these quantities. Figure 9 shows the spectral densities for each of these quantities, at each frequency, plotted against each other. The relationship is very close to being linear and therefore a linear function can be used to predict the dissipation on the basis of the known spectrum $F_i(f)$ as shown in Fig. 10:

$$S_{ds} = g\frac{\Delta F(f)}{\Delta t} = -0.0020[gF_i(f)]^{1.01} \approx -0.0016gF_i(f). \tag{17}$$

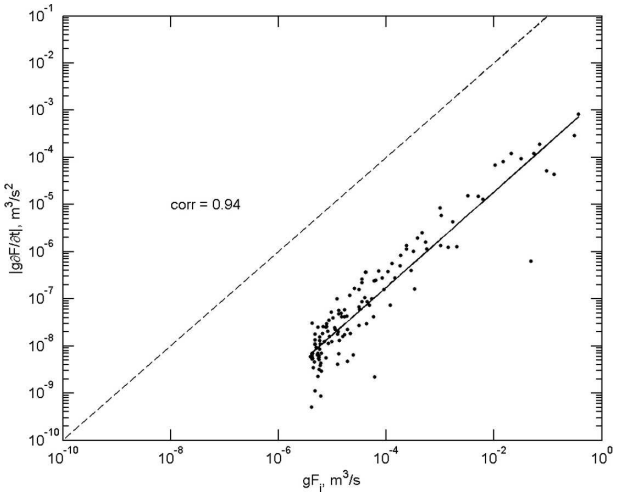

FIG. 9. Spectral difference $[\Delta F(f)]/\Delta t$ vs incipient-breaking spectrum $F_i(f)$ and linear dependence in (17). Dashed line is the line of perfect agreement.

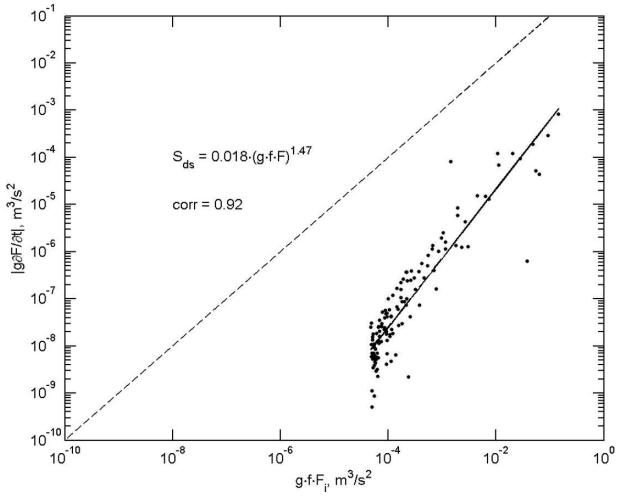

FIG. 11. Same as in Fig. 10, but vs $fF_i(f)$ and dependence in (18). Dashed line is the line of perfect agreement.

Equation (17) illustrates the linear relationship, but the proportionality coefficient is dimensional and therefore the dependence is not generally applicable. The time scale, relating the spectral derivative $S_{ds} = g[\partial F(f)]/\partial t$ and the spectrum $gF(f)$ is often assumed to be the local frequency f [e.g., (9) of Donelan 2001], and therefore the following dependence was considered:

$$S_{ds}(f) = g\frac{\Delta F(f)}{\Delta t} \sim -[gfF_i(f)]^n. \tag{18}$$

Such a dependence is nonlinear as seen in Fig. 11 where $n = 1.47$ [the right-hand side of (18) can be made to have the same dimension as S_{ds} by using the saturation spectrum $B(k)$ such as in (9)].

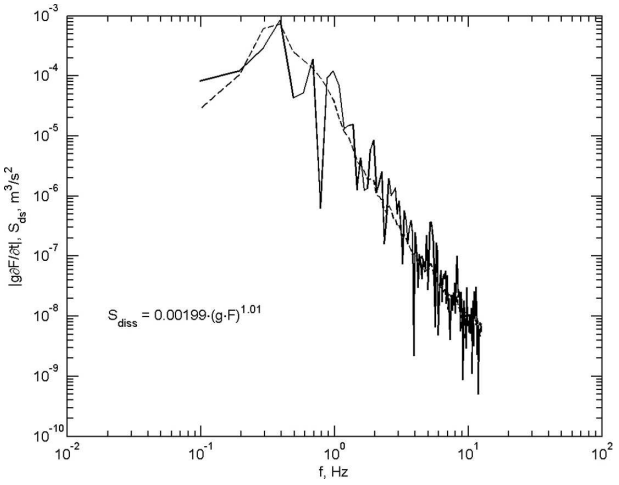

FIG. 10. Spectral difference $[\Delta F(f)]/\Delta t$ (solid line) and S_{ds} predicted by means in (17) (dashed line).

The dependence of the dissipation on the wave spectrum is, however, incomplete without taking into account the directional spreading of the waves (e.g., Young and Banner 1992; Banner and Young 1994). It is well known that at frequencies above the spectral peak the directional spreading broadens (Young et al. 1996; Babanin and Soloviev 1998b, among others). According to Banner et al. (2002), this affects the breaking threshold and therefore breaking probability at different frequencies. To achieve a universal-across-the-spectrum breaking-threshold parameter in terms of the saturation spectrum $B(k)$, Banner et al. (2002) had to normalize the saturation by a directional spectrum width.

If the breaking probability expressed in terms of the saturation spectrum $B(k)$ depends on the directional width, so should the dissipation in terms of $B(k)$ or $F(f)$. Therefore we introduced a directional-width normalization. As a measure of the inverse directional width, $A(f)$, the integral of the directional spectrum was used (Babanin and Soloviev 1998b):

$$A(f)^{-1} = \int_{-\pi}^{\pi} K(f, \theta)\, d\theta, \tag{19}$$

where $K(f, \theta)$ is the distribution of wave spectral density at frequency f along direction θ, normalized by its maximal value at this frequency:

$$K(f, \theta_{max}) = 1. \tag{20}$$

The integral width $A(f)$ has the advantage of not relying on a choice of directional-spread shape and can be easily represent in terms of such parameterizations

[e.g., s in (22)–(23); Babanin and Soloviev 1998b]. For the present application, the finite-depth directional parameterization of Young et al. (1996) was used

$$s = \begin{cases} 11.5\left(\dfrac{U_{10}}{c_p}\right)^{-2.5}\left(\dfrac{f}{f_p}\right)^{5} & f < f_p \\ 11.5\left(\dfrac{U_{10}}{c_p}\right)^{-2.5}\left(\dfrac{f}{f_p}\right)^{-2.5} & f \geq f_p, \end{cases} \quad (21)$$

where c_p is the phase speed at frequency f_p and s is the Longuet-Higgins et al. (1963) directional shape exponent:

$$K(f, \theta) = \cos^{2s(f)}\frac{\theta - \theta_{\max}}{2}. \quad (22)$$

Here $s(f)$ was then converted into $A(f)$ (Babanin and Soloviev 1998b):

$$A = \frac{\Gamma(s+1)}{2\pi^{(1/2)}\Gamma\left(s + \dfrac{1}{2}\right)}. \quad (23)$$

The dependence of the dissipation on the directionally normalized spectrum is essentially linear as seen in Fig. 12:

$$S_{\rm ds} = g\frac{\Delta F(f)}{\Delta t} = -0.0050[gfF_i(f)A(f)]^{1.12} \approx -0.0018gfF_i(f)A(f). \quad (24)$$

As above, the approximate coefficients 0.0018 was obtained by requiring the linear dependence $S_{\rm ds} = agfFA + b$ to pass through the origin (i.e., enforcing $b = 0$, or $S_{\rm ds} = 0$ at $F = 0$). The resulting coefficient is, however, much smaller than the value of 0.0050 provided by the nearly linear $S_{\rm ds} \sim 0.0050F^{1.12}$. This indicates that the requirement that $S_{ds} = 0$ at $F = 0$ is not valid. In fact, an extrapolation of Fig. 12 shows that $S_{\rm ds}$ will become zero well before the spectrum F becomes zero.

This latter fact is in good agreement with recent findings by Banner et al. (2000, 2002) and Babanin et al. (2001). As mentioned above, these studies found that there is a spectral threshold below which no breaking (and therefore no dissipation) occurs even though the spectral density is finite. In terms of such a threshold $F_{\rm thr}(f)$, the dissipation can be expressed as

$$S_{\rm ds}(f) = g\frac{\Delta F(f)}{\Delta t} \sim -gf[F_i(f) - F_{\rm thr}(f)]^n. \quad (25)$$

A quantitative expression for the threshold $F_{\rm thr}(f)$ is not known, and to evaluate its impact the postbreaking spectrum $F_p(f)$ was chosen as a threshold. Figure 13 shows the ratio of $|(\Delta F(f)/\Delta t)|$ to $[F_i(f) - F_p(f)]A(f)$. The ratio is approximately constant across the spectrum and therefore a linear dependence ($n = 1$) is expected in (25). Figure 14 shows the two spectral densities plotted versus each other at each frequency, and this relationship is indeed very close to being linear. The linear function can be used to predict the dissipation on the basis of the known spectral difference $[F_i(f) - F_p(f)]A(f)$ as shown in Fig. 15:

$$S_{\rm ds} = g\frac{\Delta F(f)}{\Delta t} = -0.0067\{gf[F_i(f) - F_p(f)]A(f)\}^{0.99} \approx -0.0065gf[F_i(f) - F_p(f)]A(f). \quad (26)$$

The exact-fit coefficient 0.0067 and the enforced linear-fit coefficient 0.0065 are very similar and demonstrate that both the assumption (25) and the choice of the

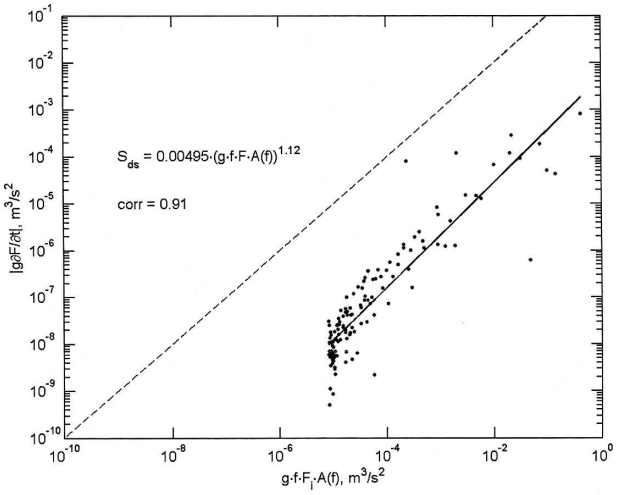

FIG. 12. Same as in Fig. 10, but vs $fF_i(f)A(f)$ and dependence (24). Dashed line is the line of perfect agreement.

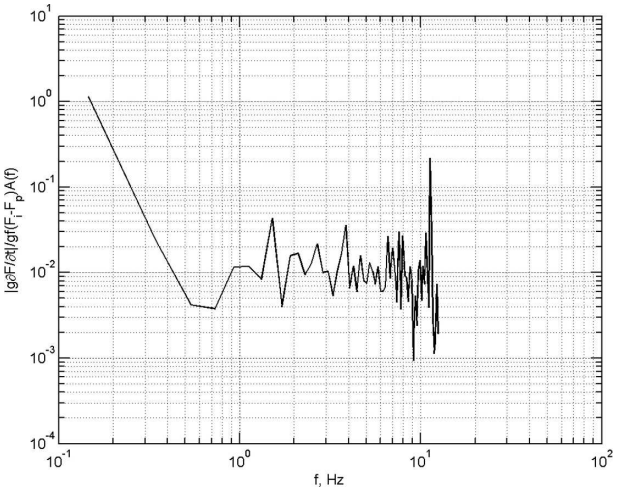

FIG. 13. Ratio of $\Delta F(f)/\Delta t$ to $f[F_i(f) - F_p(f)]A(f)$ across the spectrum.

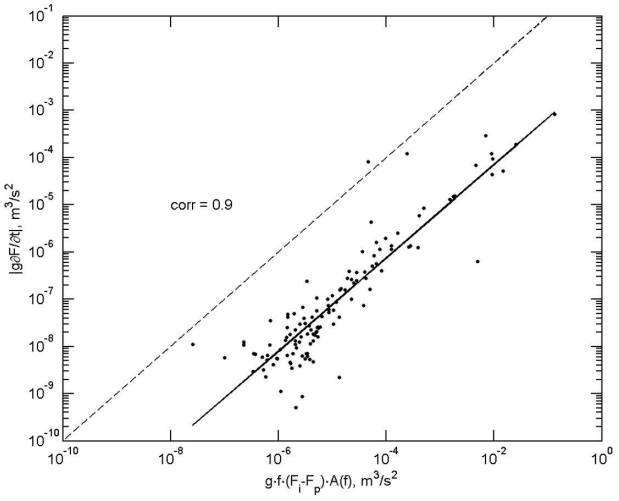

FIG. 14. Same as in Fig. 10, but vs $f[F_i(f) - F_p(f)]A(f)$. Dashed line is the line of perfect agreement.

spectral threshold are reasonable. The present choice of the spectral threshold, as the postbreaking spectrum, is academic and cannot be used for practical applications and for modeling. This threshold has to be obtained from an experiment or, currently, can be treated as a tuning parameter in the models.

5. Spectral dissipation due to dominant breaking in the directional domain

The least known feature of the spectral dissipation function is its directional behavior. The waves are directional, as are all the source functions in (1). Therefore, some directional shape, usually unimodal, must be assumed for the dissipation term. There is, however, little, if any, experimental validation of this directional shape.

The segmenting method can be used to obtain incipient-breaking and postbreaking directional spectra, similar to that used to obtain incipient-breaking and postbreaking omnidirectional spectra in section 4 above. The maximum likelihood method (MLM) developed originally by Capon (1969; see Young 1994; Young et al. 1996; Babanin and Soloviev 1998b) was used to analyze the wave array data.

It was noted that the main wave propagation direction $\theta_{\max}$ changes from segment to segment (in Fig. 16 it is shown for the spectral peak frequency f_p). This scatter around the mean main direction appeared random, not connected to whether the segment consisted of breaking or of nonbreaking waves. Therefore, the nonnormalized directional spectra $\phi(f_p, \theta)$ were obtained for each of the segments and rotated to have the same main direction ($\theta_{\max} = 0$ in Fig. 17). In Fig. 17, the solid line designates the mean incipient-breaking directional spectrum $\phi_i(f_p, \theta)$ at the spectral peak, and the dotted line shows the mean postbreaking directional spectrum $\phi_p(f_p, \theta)$. Clearly, the major energy loss occurs at angles oblique to the main propagation direction.

Figure 18 shows the ratio of the $\phi_i(f_p, \theta)$ and $\phi_p(f_p, \theta)$ spectra. Qualitatively, this ratio reflects the directional behavior of the dissipation at the spectral peak. It is unimodal, but contrary to existing assumptions, the energy loss in the main propagation direction is a minimum, with the loss increasing with direction. The impact of the dominant breaking on the directional dissipation at $2f_p$ is similar, though less pronounced (Figs. 19 and 20).

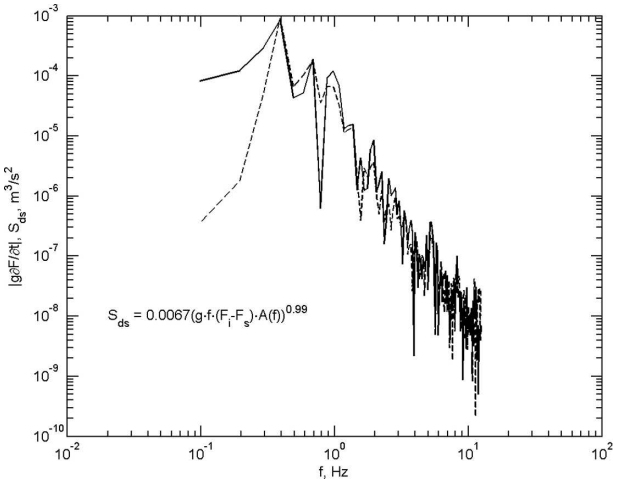

FIG. 15. Spectral difference $\Delta F(f)/\Delta t$ (solid line) and S_{ds} predicted by means in (26) (dashed line).

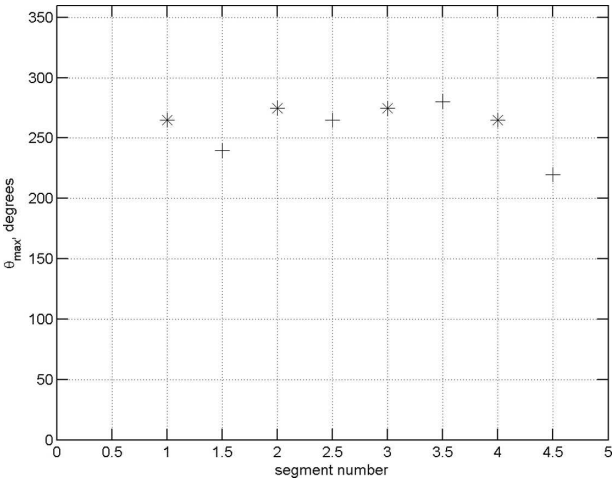

FIG. 16. Main direction of subsequent breaking wave (*) and broken wave (+) segments.

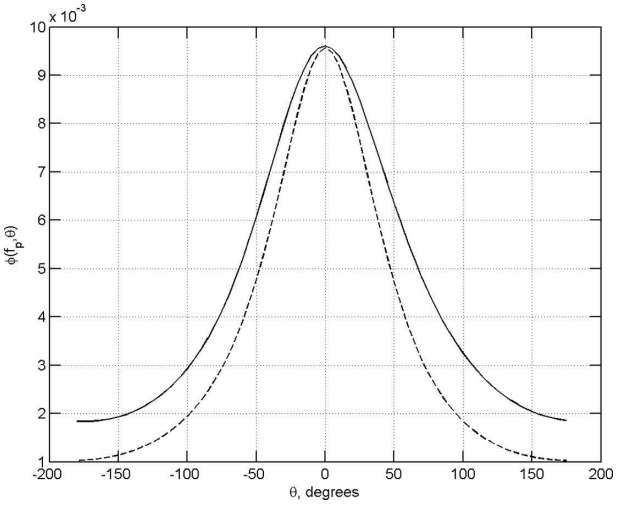

FIG. 17. Nonnormalized incipient-breaking $\phi_i(f_p, \theta)$ (solid line) and postbreaking $\phi_p(f_p, \theta)$ (dashed line) directional spectrum at peak frequency f_p. Units of the MLM directional distributions are arbitrary.

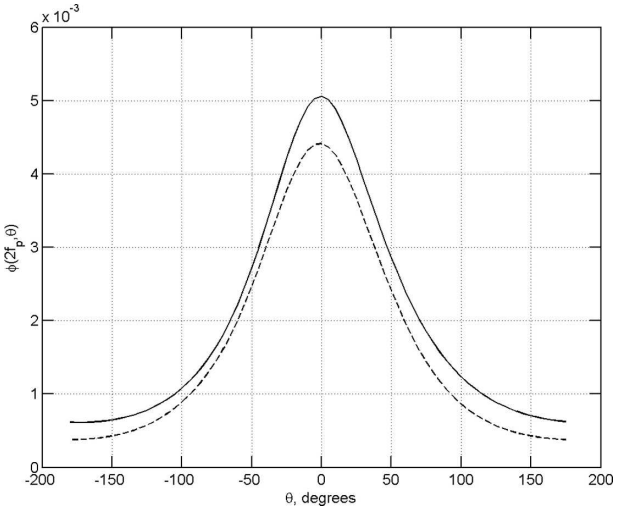

FIG. 19. Same as in Fig. 17, but for $\phi_i(2f_p, \theta)$ (solid line) and $\phi_p(2f_p, \theta)$ (dashed line) directional spectrum at double peak frequency $2f_p$.

6. Conclusions

The spectral dissipation function S_{ds} of (1), as described in section 1, is the least understood of the major source terms. Previous attempts to represent the term were indirect, based on interpreting known wave properties either prior or after wave breaking.

In the present paper, we attempted to directly estimate the spectral impact due to the breaking of dominant waves. It is argued in sections 2 and 3 that our segmenting approach should be able to provide a lower-bound estimate of such dissipation.

The main conclusion of the study is that the dominant breaking causes energy dissipation throughout the entire spectrum at scales smaller than the spectral peak waves. The dissipation rate at each frequency is linear in terms of the wave spectral density at that frequency less a spectral threshold value, with a correction for the directional spectral width. The spectral dissipation source term can be represented by

$$S_{ds}(f) = agfX[F(f) - F_{thr}(f)] + bg\int_{f_p}^{f} [F(q) - F_{thr}(q)]A(q)\,dq. \quad (27)$$

Here, the integral reflects a contribution to the dissipation at each frequency f_r of waves breaking at frequencies $f_p \le f < f_r$, and $X[F(f) - F_{thr}(f)]$ is a yet unknown

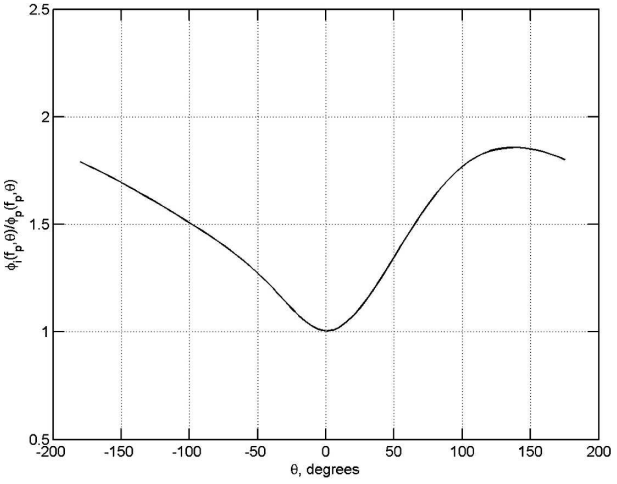

FIG. 18. Ratio of incipient-breaking $\phi_i(f_p, \theta)$ (solid line) and postbreaking $\phi_p(f_p, \theta)$ (dashed line) directional spectra at peak frequency f_p.

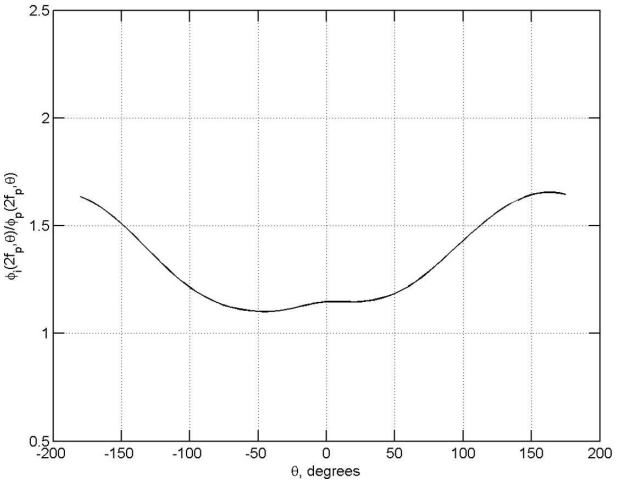

FIG. 20. Same as in Fig. 18, but for $\phi_i(2f_p, \theta)$ (solid line) and $\phi_p(2f_p, \theta)$ (dashed line) directional spectra at double peak frequency $2f_p$.

function that controls inherent wave breaking at each frequency [perhaps a function of the form described by (25)]. The coefficient a in (27) is an experimental parameter, not necessarily the constant 0.0065 determined in (26), as this parameter may be also dependent on environmental conditions (we should remember that only a single record was analyzed in the present paper).

Another important conclusion of the paper pertains to the directional properties of the dissipation. It was found that directional dissipation rates at oblique angles are higher than the dissipation in the main wave propagation direction.

Acknowledgments. The authors gratefully acknowledge the financial support of the U.S. Office of Naval Research (Grants N00014-97-1-0234, N00014-97-1-0277, and N00014-97-1-0233) and the Australian Research Council (Grant A00102965). We also express our gratitude to the staff of the School of Civil Engineering of the Australian Defence Force Academy: Jim Baxter, Michael Jones, Mary Dalton, Michael Lanza, John MacLeod, Bernard Miller, Karl Shaw, Ian Shepherd, and Michael Wilson, who offered highly professional help during the Lake George experiment.

REFERENCES

Agrawal, Y. C., E. A. Terray, M. A. Donelan, P. A. Hwang, A. J. Williams III, W. M. Drennan, K. K. Kahma, and S. A. Kitaigorodskii, 1992: Enhanced dissipation of kinetic energy beneath surface waves. *Nature,* **359,** 219–220.

Arsenyev, S. A., S. V. Dobroklonsky, R. M. Mamedov, and N. K. Shelkovnikov, 1975: Direct measurements of some characteristics of fine-scale turbulence from a stationary platform in the open sea. *Izv. Atmos. Oceanic Phys.,* **11,** 530–533.

Babanin, A. V., and Y. P. Soloviev, 1998a: Field investigation of transformation of the wind wave frequency spectrum with fetch and the stage of development. *J. Phys. Oceanogr.,* **28,** 563–576.

——, and ——, 1998b: Variability of directional spectra of wind-generated waves, studied by means of wave staff arrays. *Mar. Freshwater Res.,* **49,** 89–101.

——, I. R. Young, and M. L. Banner, 2001: Breaking probabilities for dominant surface waves on water of finite constant depth. *J. Geophys. Res.,* **106,** 11 659–11 676.

Banner, M. L., and I. R. Young, 1994: Modeling spectral dissipation in the evolution of wind waves. Part I: Assessment of existing model performance. *J. Phys. Oceanogr.,* **24,** 1550–1571.

——, I. S. F. Jones, and J. C. Trinder, 1989: Wavenumber spectra of short gravity waves. *J. Fluid Mech.,* **198,** 321–344.

——, A. V. Babanin, and I. R. Young, 2000: Breaking probability for dominant waves on the sea surface. *J. Phys. Oceanogr.,* **30,** 3145–3160.

——, J. R. Gemmrich, and D. M. Farmer, 2002: Multi-scale measurements of ocean wave breaking probability. *J. Phys. Oceanogr.,* **32,** 3364–3375.

Capon, J., 1969: High-resolution frequency-wavenumber spectrum analysis. *Proc. IEEE,* **57,** 1408–1418.

Dillon, T. M., J. G. Richman, C. G. Hansen, and M. D. Pearson, 1981: Near-surface turbulence measurements in a lake. *Nature,* **290,** 390–392.

Donelan, M. A., 2001: A nonlinear dissipation function due to wave breaking. *Proc. ECMWF Workshop on Ocean Wave Forecasting,* Reading, United Kingdom, ECMWF, 87–94.

——, and W. J. Pierson, 1987: Radar scattering and equilibrium ranges in wind-generated waves with application to scatterometry. *J. Geophys. Res.,* **92,** 4971–5029.

——, and Y. Yuan, 1994: Wave dissipation by surface processes. *Dynamics and Modelling of Ocean Waves,* G. J. Komen et al., Eds., Cambridge University Press, 143–155.

——, M. S. Longuet-Higgins, and J. S. Turner, 1972: Whitecaps. *Nature,* **239,** 449–451.

——, J. Hamilton, and W. H. Hui, 1985: Directional spectra of wind-generated waves. *Philos. Trans. Roy. Soc. London,* **315A,** 509–562.

——, A. V. Babanin, I. R. Young, and M. L. Banner, 2006: Wave follower field measurements of the wind input spectral function. Part II: Parameterization of the wind input. *J. Phys. Oceanogr.,* in press.

Drennan, W. M., M. A. Donelan, E. A. Terray, and K. B. Katsaros, 1996: Oceanic turbulence dissipation measurements in SWADE. *J. Phys. Oceanogr.,* **26,** 808–815.

Feng, H., and Y. Yeli, 1992: Theoretical study of breaking wave spectrum and its application. *Breaking Waves—IUTAM Symposium,* M. L. Banner and R. H. J. Grimshaw, Eds., Springer-Verlag, 277–282.

Gemmrich, J. R., and D. M. Farmer, 2004: Near-surface turbulence in the presence of breaking waves. *J. Phys. Oceanogr.,* **34,** 1067–1086.

Hanson, J. L., and O. M. Phillips, 1999: Wind sea growth and dissipation in the open ocean. *J. Phys. Oceanogr.,* **29,** 1633–1648.

Hara, T., and S. E. Belcher, 2002: Wind forcing in the equilibrium range of wind-wave spectra. *J. Fluid Mech.,* **470,** 223–245.

Hasselmann, K., 1960: Grundgleichungen der Seegangsvoraussage [The fundamental equations of sea-state prediction]. *Schiffstechnik,* **7,** 191–195.

——, 1962: On the non-linear energy transfer in a gravity-wave spectrum. Part I. General theory. *J. Fluid Mech.,* **12,** 481–500.

——, 1974: On the spectral disspation of ocean waves due to white capping. *Bound.-Layer Meteor.,* **6,** 107–127.

Holthuijsen, L. H., and T. H. C. Herbers, 1986: Statistics of breaking waves observed as whitecaps in the open sea. *J. Phys. Oceanogr.,* **16,** 290–297.

Hwang, P. A., and D. W. Wang, 2004: An empirical investigation of source term balance of small scale surface waves. *Geophys. Res. Lett.,* **31,** L15301, doi:10.1029/2004GL020080.

——, D. Xu, and J. Wu, 1989: Breaking of wind-generated waves: Measurements and characteristics. *J. Fluid Mech.,* **202,** 177–200.

Jones, I. S. F., 1985: Turbulence below wind waves. *The Ocean Surface—Wave Breaking, Turbulent Mixing and Radio Probing,* Y. Toba and H. Mitsuyasu, Eds., Reidel, 437–442.

Kahma, K. K., 1981: A study of the growth of the wave spectrum with fetch. *J. Phys. Oceanogr.,* **11,** 1505–1515.

Kitaigorodskii, S. A., 1983: On the theory of the equilibrium range in the spectrum of wind-generated gravity waves. *J. Phys. Oceanogr.,* **13,** 816–826.

Komen, G. J., L. Cavaleri, M. A. Donelan, K. Hasselmann, S. Hasselmann, and P. A. E. M. Janssen, 1994: *Dynamics and Modelling of Ocean Waves.* Cambridge University Press, 532 pp.

Kudryavtsev, V. N., and V. K. Makin, 2002: Coupled dynamics of short wind waves and the air flow over long surface waves. *J. Geophys. Res.,* **107,** 3209, doi:10.1029/2001JC001251.

Landau, L. D., and E. M. Lifshitz, 1986: *Hydrodynamics* (in Russian). Nauka, 736 pp.

Leykin, I. A., and A. D. Rozenberg, 1984: Sea-tower measurements of wind-wave spectra in the Caspian Sea. *J. Phys. Oceanogr.,* **14,** 168–176.

Liu, P. C., and A. V. Babanin, 2004: Using wavelet spectrum analysis to resolve breaking events in the wind wave time series. *Ann. Geophys.,* **22,** 3335–3345.

——, D. J. Schwab, and R. E. Jensen, 2002: Has wind-wave modeling reached its limit? *Ocean Eng.,* **29,** 81–98.

Longuet-Higgins, M. S., 1969: On wave breaking and the equilibrium spectrum of wind-generated waves. *Proc. Roy. Soc. London,* **310A,** 151–159.

——, D. E. Cartwright, and N. D. Smith, 1963: Observations of the directional spectrum of sea waves using the motions of the floating buoy. *Proceedings of the Conference on Ocean Wave Spectra,* Prentice Hall, 111–136.

Manasseh, R., A. V. Babanin, C. Forbes, K. Rickards, I. Bobevski, and A. Ooi, 2006: Passive acoustic determination of wave-breaking events and their severity across the spectrum. *J. Atmos. Oceanic Technol.,* in press.

Melville, W. K., 1994: Energy dissipation by breaking waves. *J. Phys. Oceanogr.,* **24,** 2041–2049.

——, and P. Matusov, 2002: Distribution of breaking waves at the ocean surface. *Nature,* **417,** 58–63.

——, M. R. Loewen, and E. Lamarre, 1992: Sound production and air entrainment by breaking waves: A review of recent laboratory experiments. *Breaking Waves—IUTAM Symposium,* M. L. Banner and R. H. J. Grimshaw, Eds., Springer-Verlag, 139–146.

Meza, E., J. Zhang, and R. J. Seymour, 2000: Free-wave energy dissipation in experimental breaking waves. *J. Phys. Oceanogr.,* **30,** 2404–2418.

Oakey, N. S., and J. A. Elliott, 1982: Dissipation within surface mixed layer. *J. Phys. Oceanogr.,* **12,** 171–185.

Phillips, O. M., 1958: The equilibrium range in the spectrum of wind generated waves. *J. Fluid Mech.,* **4,** 426–434.

——, 1985: Spectral and statistical properties of the equilibrium range in wind-generated gravity waves. *J. Fluid Mech.,* **156,** 505–531.

——, F. L. Posner, and J. P. Hansen, 2001: High-range resolution radar measurements of the speed distribution of breaking events in wind-generated ocean waves: Surface impulse and wave energy dissipation rates. *J. Phys. Oceanogr.,* **31,** 450–460.

Polnikov, V. G., 1993: On a description of a wind-wave energy dissipation function. *The Air–Sea Interface: Radio and Acoustic Sensing, Turbulence and Wave Dynamics,* M. A. Donelan, W. H. Hui, and W. J. Plant, Eds., Rosenstiel School of Marine and Atmospheric Science, University of Miami, 277–282.

Rapp, R. J., and W. K. Melville, 1990: Laboratory measurements of deep-water breaking waves. *Philos. Trans. Roy. Soc. London,* **331A,** 735–800.

Skafel, M. G., and M. A. Donelan, 1997: Laboratory measurements of stress modulation by wave groups. *Geophysica,* **33,** 9–14.

Soloviev, A. V., and R. Lukas, 2003: Observation of wave-enhanced turbulence in the near-surface layer of the ocean during TOGA COARE. *Deep-Sea Res.,* **50A,** 371–395.

——, N. V. Vershinsky, and V. A. Bezverchnii, 1988: Small-scale turbulence measurements in the thin surface layer of the ocean. *Deep-Sea Res.,* **35,** 1859–1874.

Terray, E. A., M. A. Donelan, Y. C. Agrawal, W. M. Drennan, K. K. Kahma, A. J. Williams III, P. A. Hwang, and S. A. Kitaigorodskii, 1996: Estimates of kinetic energy dissipation under breaking waves. *J. Phys. Oceanogr.,* **26,** 792–807.

Thorpe, S. A., 1993: Energy loss by breaking waves. *J. Phys. Oceanogr.,* **23,** 2498–2502.

Toba, Y., 1972: Local balance in the air-sea boundary processes. III. On the spectrum of wind waves. *Oceanogr. Soc. Japan,* **29,** 209–220.

Veron, F., and W. K. Melville, 1999: Pulse-to-pulse coherent Doppler measurements of waves and turbulence. *J. Atmos. Oceanic Technol.,* **16,** 1580–1597.

Young, I. R., 1994: On the measurement of directional wave spectra. *Appl. Ocean Res.,* **16,** 283–294.

——, and M. L. Banner, 1992: Numerical experiments on the evolution of fetch limited waves. *Breaking Waves—IUTAM Symposium,* M. L. Banner and R. H. J. Grimshaw, Eds., Springer-Verlag, 267–275.

——, and L. A. Verhagen, 1996: The growth of fetch limited waves in water of finite depth. Part 1. Total energy and peak frequency. *Coastal Eng.,* **29,** 101–121.

——, ——, and S. K. Khatri, 1996: The growth of fetch limited waves in water of finite depth. Part 3. Directional spectra. *Coastal Eng.,* **29,** 47–78.

——, M. L. Banner, M. A. Donelan, A. V. Babanin, W. K. Melville, F. Veron, and C. McCormic, 2005: An integrated system for the study of wind-wave source terms in finite-depth water. *J. Atmos. Oceanic Technol.,* **22,** 814–831.

Yuan, Y., C. C. Tung, and N. E. Huang, 1986: Statistical characteristics of breaking waves. *Wave Dynamics and Radio Probing of the Ocean Surface,* O. M. Phillips and K. Hasselmann, Eds., Plenum, 265–272.

Zakharov, V. E., 1966: Some aspects of nonlinear theory of surface waves (in Russian). Ph.D. thesis, Institute for Nuclear Physics, Novosibirsk, Russia.

——, 1968: Stability of periodic waves of finite amplitude on the surface of a deep fluid. *Zhurnal Prikladnoi Mekh. Tekknich. Fiz.,* **3,** 80–94.

——, 2002: Theoretical interpretation of fetch-limited wind-driven sea observations. Preprints, *Seventh Int. Workshop on Wave Hindcasting and Forecasting,* Banff, AB, Canada, 286–295.

——, and N. Filonenko, 1967: The energy spectrum for stochastic oscillations of a fluid surface. *Sov. Phys. Docl.,* **11,** 881–884.

——, and A. V. Smilga, 1981: About quasi-one dimensional spectra of weak turbulence (in Russian). *Zurnal Eksp. Teor. Fiz.,* **81,** 1318–1327.

——, and M. M. Zaslavskii, 1982a: Kinetic equation and Kolmogorov spectra in weak-turbulence theory of wind-generated waves. *Izv. Atmos. Oceanic Phys.,* **18,** 970–980.

——, and ——, 1982b: Integrals of input and dissipation in the weak-turbulence theory of wind-generated waves. *Izv. Atmos. Oceanic Phys.,* **18,** 1066–1076.

——, and ——, 1983a: Shape of spectrum of energy carrying components of a water surface in the weak-turbulence theory of wind waves. *Izv. Atmos. Oceanic Phys.,* **19,** 207–212.

——, and ——, 1983b: Dependence of wave parameters on the wind velocity, duration of its action and fetch in the weak-turbulence theory of water waves. *Izv. Atmos. Oceanic Phys.,* **19,** 300–306.